RESEARCH PAPER

ANALYSING THE EFFECT OF THERMAL TREATMENT WITH THE AID OF BRINE QUENCHING ON MICROSTRUCTURAL CHARACTERISTICS AND PHYSICAL PROPERTIES OF AISI-304 PLATES

Saurabh Dewangan[1], Gopal Sukhwal[1]*

[1] Department of Mechanical Engineering, Manipal University Jaipur, Jaipur, Rajasthan, India, Pin-303007

*Corresponding author: gopalsukhwal352@gmail.com, Tel.: 0141-3999100, Department of Mechanical Engineering, Manipal University Jaipur, Jaipur, Rajasthan, India, Pin-303007.

ABSTRACT

In this work, the effects of brine quenching on the mechanical properties and microstructural attributes of AISI 304 steel have been analyzed. For reference purposes, one sample was kept in an 'as-received' condition. Three steel plates were treated at 800ºC for holding periods of 1 hour, 1.5 hours, and 2 hours respectively. The heated samples were cooled inside the brine solution up to room temperature. For mechanical property analysis, all four plates were cut into standard-sized specimens for the tensile test, hardness test, and toughness test. The microstructural analysis reveals that pitting corrosion has affected the γ-grains as well as δ-boundaries. The 'as-received' sample has shown the highest value of ultimate tensile strength (UTS) i.e., 940 MPa with 59.5% of elongation whereas the third heat-treated sample, which was heated for 2 hours, has shown a decrement of 13% and 55% in UTS and elongation respectively as compared to these of 'as received' sample. As a result of Cr-deterioration and carbide dissolution at grain boundaries, an increase in hardness was recorded in the heat-treated samples. Also, the lowest toughness, 35% lower than the as-received sample, was recorded in the third sample which are heated for a long period.

Keywords: AISI-304; Quenching; Brine solution; Tensile strength; Toughness; Hardness; Microstructure; FESEM; XRD

INTRODUCTION

Stainless steel is an iron-based alloy having at least 10.5 % of chromium content which makes it strong and highly corrosion-resistant as compared to other types of steel. Besides Fe and C, other important elements like Ni, Mn, Mo, and N are commonly alloyed in stainless steel [1]. Other favorable properties of stainless steel are its thermal resistivity, formability, easy-to-fabricate, attractive polished appearance, and environmental friendly [2]. For stainless steel, numerical grading systems are designated according to their composition, physical properties, and applications. Stainless steel (SS) can be divided into four categories: ferritic, martensitic, austenitic, and austenitic+ferritic (or duplex) SS. These steels can be distinguished according to their microstructural appearance at room temperature [3]. Although SS is known for its corrosion-resistant properties, other properties like fracture toughness and oxidative resistance can be altered by the addition of other alloying elements. For example, Nb and Ti improve the IGC (inter-granular corrosion) resistance property of SS by absorbing the carbon to form carbides [4]. Machinability is enhanced by sulfur which is responsible to form manganese sulfide [5]. Nitrogen helps to improve the strength of the steel [6]. Because of its good surface finish and anti-corrosion properties, SS is used in various industries like chemical, aerospace, medical, pharmaceutical, food processing, and even household as well as jewelry works [7].

Several works on the effect of varying thermal treatment on stainless steel were done in recent past years. The literature review is summarized here.

In a research work, the optical microscopy, tensile test, and hardness test have been done to measure the mechanical property after quenching heat treatment on SS. The result shows that the hardness is reduced, and the strength and elongation are increased after-heat treatment [8]. The tube hydroforming process has been simulated for SS-304 steel for various heat-treated conditions. The forming limit curve (FLC) of SS – 304 at different temperatures of annealing i.e., 150˚ C, 200ºC, and 250ºC have been analyzed and compared with the original condition. With the help of the numerical simulation method, it has been found that the annealed temperature has a significant impact on the FLC of the hydroformed tube. By increasing the temperature up to 200ºC, an increment of FLC has been recorded while it has slightly decreased at a temperature level of 250ºC [9]. Clinching is the process of joining metals without welding but with the aid of external force to produce plastic deformation. The effect of heat treatment on the mechanical properties of the clinched joint of SS 304 has been investigated in a work. With the help of classical metallography and advanced SEM technique, distinguish joints made from non-thermal treated and thermal-treated sheets have been analyzed. A significant impact of heat treatment on the surface roughness and strength of the joint has been observed [10]. When stainless steels are exposed to high temperatures around 470-750ºC, it becomes sensitized due to carbide precipitation at grain boundaries. Carbide precipitation can have a harmful effect on the resistance to intergranular corrosion which further can reduce the tensile properties of SS, specifically strength and toughness. In a research work, standard-sized tensile and hardness test specimens of SS-304 have been subjected to different heat treatment processes, which consist of heating at 660ºC, and then air cooling and solution annealed at five different temperatures i.e., 1010ºC, 1050ºC, 1090ºC, 1140ºC and 1190ºC and then water quenching. It has been found that the sensitized samples give the highest hardness value at 660ºC and the

solution annealed samples possess the highest hardness at 1090ºC. 1090ºC has been found to be the optimum temperature to avoid grain growth for the solution-annealed sample [11]. The impact of Thermal treatment on the microstructure and corrosion resistance of stainless/carbon steel bimetal has been investigated. The annealing has been done at 700ºC for this plate. During annealing, the diffusion of carbon has taken place from the CS (carbon steel) to SS (stainless steel) on the bimetal plate. Because of diffusion, the carbon content of SS has raised up to 0.08%. The elevated carbon content can cause a reduction of chromium on the SS surface and thereby corrosion resistance may hamper [12]. The addition of copper (Cu) has been found beneficial for reducing the microbiologically stimulated corrosion in both austenitic and duplex stainless steels [13]. The corrosion resistance of sensitized stainless steel has been analyzed under a chloride solution. As per the results obtained through multiple tests, it has been concluded that sensitization has significantly conditioned the corrosion resistance properties of the steel and too the high temperature has accelerated this process [14]. In a work, the rolling impact at room temperature on mechanical properties and microstructure of nitrogen-bearing AISI 304 austenitic steel has been analyzed. The cold rolling reductions from 5% to 90% have been used. To check the mechanical properties, hardness, and tensile tests have been carried out. With the subsequent cold rolling reduction, multiple α'- martensite grains have been observed alongside the rolling route. The formation of α'-martensite results in the massive strengthening of the metal and a significant decrease in elongation [15]. AISI 304 steel has been widely utilized for corrosion testing. Under the influence of oxidative chemicals, mainly carbide dissolution [16], intergranular corrosion [17], and pitting corrosion [18] have been reported in some previous works.

In this work, an attempt has been made to analyze the possible variation of tensile strength, hardness, toughness, and intergranular corrosive phenomena in the AISI 304 steel samples after heat treatment. The thermal treatment at 800 ºC temperature and subsequent quenching in brine solution media have been considered in this work. As per the Fe-Cr phase diagram for austenitic stainless steel, 800 ºC is an elevated temperature at which metal is recrystallized and stresses are relieved. No phase change occurs at this temperature. This means, the microstructure of SS-304 at room temperature, i.e., γ+δ will remain the same at the temperature level of 800 ºC. Many research works have applied the annealing temperature >1000 ºC for the complete phase conversion. In this work, heat treatment and further analysis have been carried out keeping the phases unchanged.

MATERIAL AND METHODS

Four nos. of AISI-304 steel samples with the approximate dimension of 130×75×2 mm were taken in this study. Samples were named A, B, C, and D. First one, i.e., sample A was kept in the 'as received' condition while three others were undergone the thermal treatment process. Treatment involves heating the samples into an induction furnace up to a temperature of 800ºC. Sample B was heated for 1 hr and then cooled in a brine solution. Sample C and Sample D were heated for 1.5 hr and 2 hr respectively and then cooled in brine solution like Sample B. All the four samples under study are shown in **Fig. 1**.

The tensile test specimens were cut from each plate as per ASTM standards. For that, the Wire-EDM machine was utilized under study. A universal testing machine with 40kN capacity was used for tensile testing. A common strain rate of 0.002 s^{-1} was fixed for each sample prior to testing. The fractured tensile specimens are shown in **Fig. 2**.

For the hardness test, Rockwell (C-scale) hardness tester was taken into consideration. A total of four indents at different locations were made and an average value of hardness was calculated for each plate.

To know the toughness variation in the plate at pre- and post-heat-treated conditions, the Charpy impact test was conducted in the study. From each plate, two specimens were prepared for the Charpy test. The size of each specimen was 60×10×2 mm. At the center position of the specimen, a deep 'U' notch with a 4 mm depth was cut off. The orientation of the impact hammer was 135º from the vertical position from where it was suspended to hit the sample.
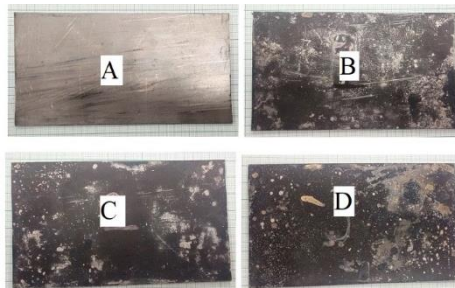
Fig. 1 Heat treatment process; Sample A- as received; Sample B- heated and held up to 800 ºC for 1 hr; Sample C- heated and held up to 800 ºC for 1.5 hr; Sample D- heated and held up to 800 ºC for 2 hr
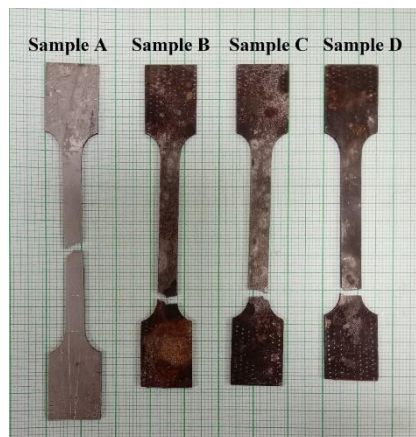
Fig. 2 Fractured specimens after tensile test

All four samples were properly polished by using a polishing machine. Water and very fine alumina were applied on the rotating surfaces to give them a mirror-like appearance. Kalling (No-2) reagent was used as an etchant for microstructural observation. The four polished specimens are shown in **Fig. 3**.
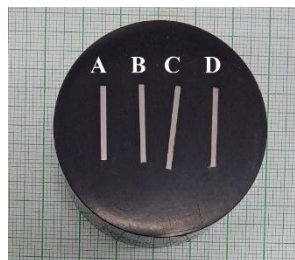
Fig. 3 Four polished specimens for microstructural analysis

RESULT ANALYSIS

Tensile test results: At first, sample A was tested because its values are taken as a reference for other samples. Sample A had shown a UTS of 940 MPa at a maximum loading of 7.3 kN. The YS (0.2% proof strength) of the sample was 518 MPa. A total elongation of 59.5% was recorded in the sample prior to fracture. Sample B, heated for 1 hr, had shown a decrement of 6% in UTS value (883 MPa). As a result of heating, Cr might have been severely affected and hence the ductility of the sample got significantly reduced by 50%, although a comparable result was obtained for YS. Sample C, which was heated for 1.5 hr, carries a UTS value of 832 MPa which is nearly 11% lesser than that of sample A. This means a long holding time has a more negative effect on UTS. The elongation in sample C was reported nearly 50% lower than that of sample A. Sample D was heated for a period of 2 hr and then cooled in brine. Its UTS and YS were measured as 814 MPa and 511 MPa respectively. As compared to sample A, the UTS and YS of sample D are 13% and 1% lower. The UTS is minimum in sample D. Also, the elongation, a measure of ductility, has been reported with a 55% reduction. The analysis of tensile test results establishes that thermal treatment and brine cooling has sensitized the SS-304 samples. Due to this, Cr-embrittlement has occurred which further has led to a reduction of UTS and ductility. The main results obtained by the tensile test are written in **Table 1**. For each plate, load-displacement graphs are shown in **Fig. 4** (a, b, c, d). Also, a comparative analysis among UTS, YS, and elongation is shown in Fig. 4 (e, f).

Table 1 The outcomes of tensile testing of four plates

Sample	UTS (MPa)	UTL (kN)	YS/0.2% PS (MPa)	YS/0.2% PL (kN)	% Elongation
1	940	7.3	518	4	59.5
2	883	6.9	506	4	29.5
3	832	6.4	501	3.8	30
4	814	6.3	511	4	26.5

(a)

(b)

(c)

(d)

(e)

(f)
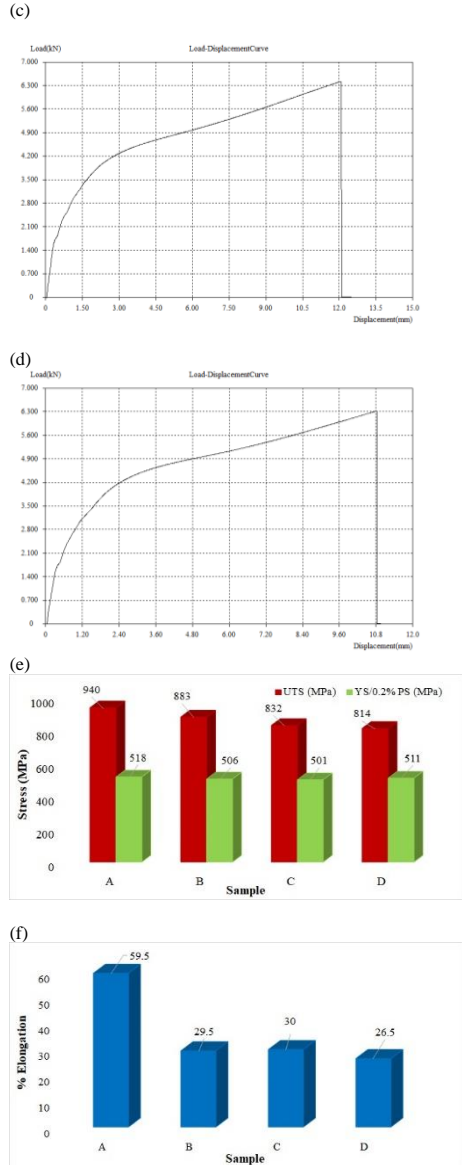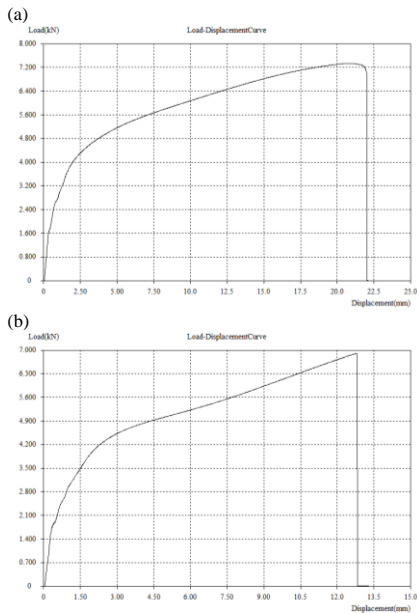
Fig. 4 Load-displacement graphs after the tensile test: (a) Sample-A; (b) Sample-B; (c) Sample-C; (d) Sample-D; (e) Comparison among UTS and YS; (f) Comparison among % elongation

Hardness test results: As mentioned above, an average value of hardness was determined. The results confirm that sample A, an untreated sample, possesses the least hardness value of 26 HRC whereas the values get increased with increasing the holding time. Sample B, C, and D have shown the hardness of 29 HRC, 30 HRC, and 39 HRC respectively. These values are nearly 12%, 15%, and 50% higher than the hardness of sample A. The comparative bar chart is given in **Fig. 5**.
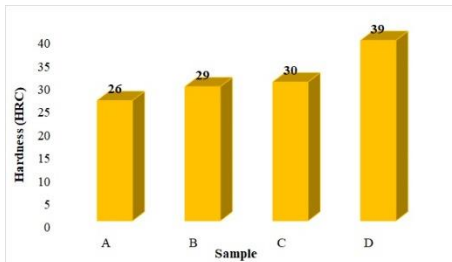
Fig. 5 (a) Rockwell hardness testing of samples; (b) Comparison among hardness of different samples

Toughness test results: The specimens for the toughness test are shown in **Fig. 6** (a). The impact hammer of the toughness test specimen was fallen freely twice to check for any error. The reported error of 3 J was subtracted from the observed value in each sample. From each plate, two specimens were prepared for this test and an average toughness was calculated by using the observations of both specimens. The toughness values observed in each specimen are written in **Table 2**. The used/fractured specimens are shown in Fig. 6 (b). Also, the comparison of their toughness is shown by using a bar chart (Fig. 6c).

Table 1 Toughness test results

Sample	Test No	Toughness values (J)	Average Toughness (J)
A	1	10	10
	2	10	
B	1	8	9
	2	10	
C	1	6	7.5
	2	9	
D	1	6	6.5
	2	7	
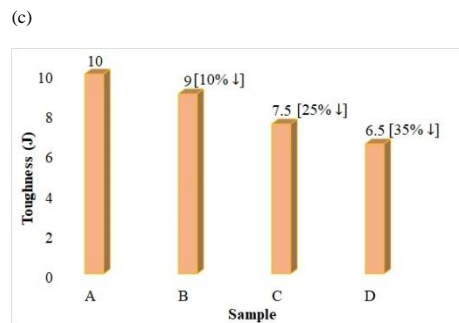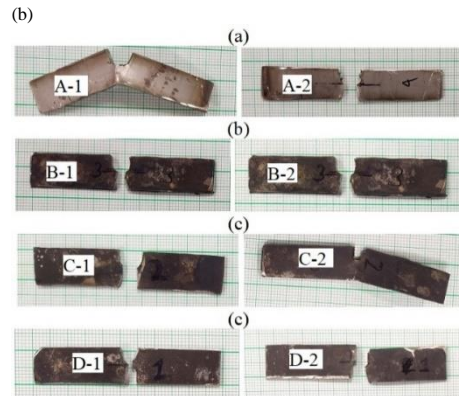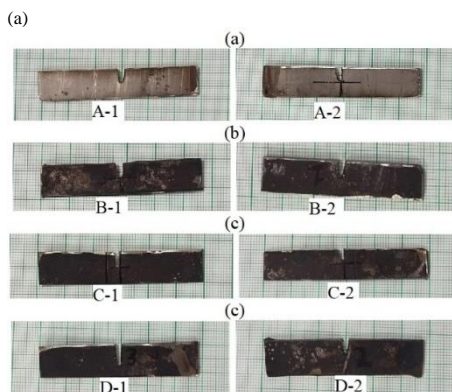
Fig. 6 (a) Charpy impact test specimens; (b) Fractured specimens after test; (c) Comparative analysis among toughness values

Microstructure analysis: The microstructure of the steel samples was observed at a magnification of 500X and at a common scale of 50 μm. Sample A, an untreated sample, is in the cold-rolled state in which twins can be seen. γ and δ phases can be recognized by their color contrast. γ-matrix appears as bright-colored grains whereas δ has a darker appearance. Also, a thin black boundary between the γ-δ phase could also be observed in this sample. Metal carbides can be recognized as fine black particles dispersed throughout the γ-δ matrix. Several black-colored strings represent δ-ferrite (Fig. 7a). The microstructure of sample-A can be considered a reference for other samples to compare the results. As compared to Sample-A, other heat-treated samples possess a huge variation in the microstructure. Sample-B is possessing coarse-sized γ-grains with a thick black boundary with δ. Twins disappeared due to heating. The thick boundary is containing intergranular corrosion due to carbide dissolution according to the results obtained by [19]. The carbide dissolution occurs due to Cr-depletion [14] which further vouches the pitting corrosion in the grains (Fig. 7b). In sample-C, the grains are coarse and normally equiaxed. The sample-C has been heated for a longer time as compared with sample-B. Due to this, the width of grain boundaries is quite higher. However, grain size has not been measured in this work. Ditches, as discussed in [20], can be seen in the γ-δ boundaries. Some parts are highlighted with pitting corrosion on the grains (Fig. 7c). Sample-D, which has been heated for the longest duration, has thicker black boundaries than that of sample-B and sample-C. The grain size is also coarser than the above two samples. A clearer representation of carbide deterioration and pitting corrosion has been presented in Fig. 7(d). Besides Cr depletion, MnS inclusion can

also initiate the pitting corrosion at the intergranular boundary as discussed by [21, 22].

(a)

(b)

(c)

(d)
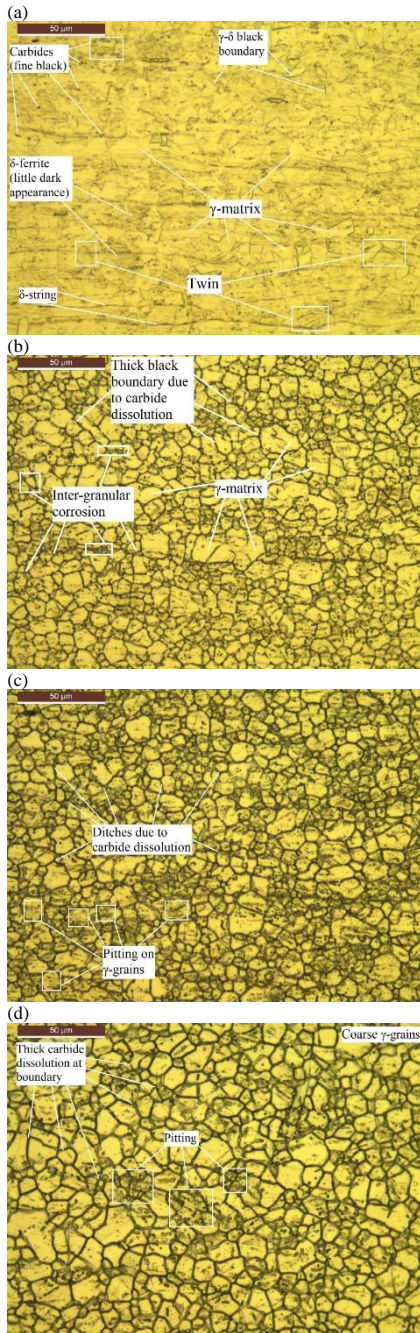
Fig. 7 Microstructural analysis of four plates: (a) Sample-A (as received); (b) Sample-B, heated for 1 hr; (c) Sample-C, heated for 1.5 hr; (d) Sample-D, heated for 2 hr

(a)

(b)

(c)
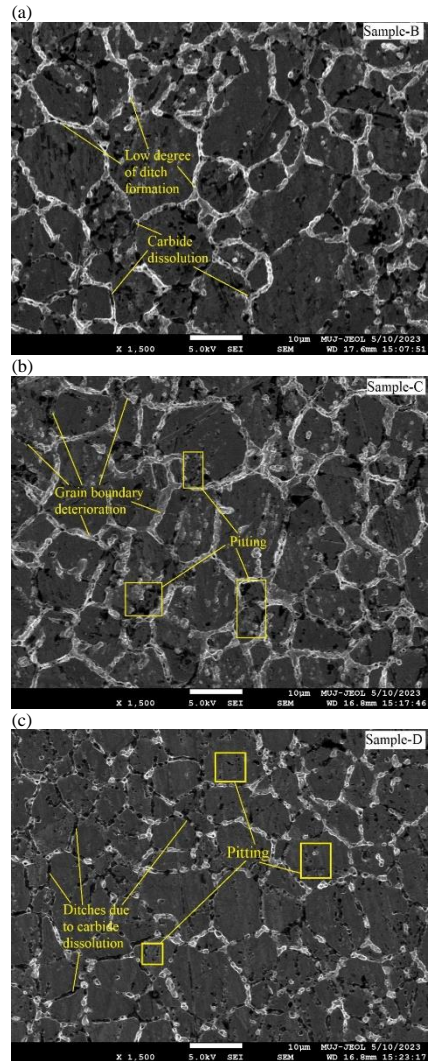
Fig. 8 Pitting and intergranular corrosion in heated samples

The intergranular corrosion in samples B, C, and D could be properly seen by FESEM images (**Fig. 8**). As soon as the holding time gets increases, the intergranular ditches become wider. It is due to the dissolution of carbide in the boundaries. The individual γ-grain possesses pitting corrosion due to brine cooling.

XRD analysis of all the specimens proves the presence of oxide in heat-treated samples. Mainly two types of oxides, named, chromium oxide (Cr_2O_3) and iron oxide (Fe_2O_3) were reported in heat-treated samples. The results of the present work have been compared with the same of Zhan et al. [23]. have been compared Cr_2O_3 was found at 13° and 25° of 2θ whereas Fe_2O_3 was reported at 2θ of 35° and 43°. Comparative XRD peaks are shown in **Fig. 9**.
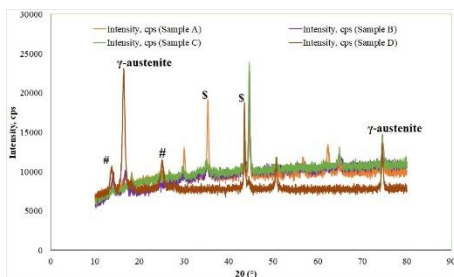
Fig. 9 XRD analysis of four samples; oxide formation can be seen along with γ-austenite (# = Cr_2O_3; $ = Fe_2O_3)

CONCLUSIONS

The following conclusions can be drawn from this study:

1. The microstructure of 304 steel mainly shows fine grain boundaries between the γ-δ phase. The appearance of γ and δ are bright and dark respectively. Also, δ is present in the form of strings. Upon heat treatment and brine cooling, sensitization has been reported, mainly at the grain boundaries. The heat-treated samples contain thick and dark black boundaries which resemble the presence of ditches due to carbide dissolution. It proves that salinity has vouched for the corrosion at grain boundaries which has further deteriorated the Cr content. As soon as the heating period increases, grain size and ditches at the grain boundary have grown in the samples. FESEM images have established the fact of ditches and pitting formation. As a result of corrosion, the formation of chromium oxide and iron oxide has been noticed by XRD.

2. The tensile strength has been negatively affected by heat treatment. The lowest strength has been seen in sample D which was heated for the longest time. It may be due to intergranular corrosion between γ-grains. The UTS reductions in sample-B, C, and D are 6%, 11%, and 13% respectively compared to sample-A. Also, the Cr-embrittlement has significantly reduced the ductility of all three samples. With respect to sample A, a decrement of 55% was noted in the ductility of sample D.

3. Heat treatment and brine cooling methods have increased the surface hardness of the samples. With increasing the holding time, hardness keeps on increasing. Sample D with 2 hr of holding time imparts nearly 50% higher hardness than that of the original sample.

4. Toughness of the untreated sample has been reported as the highest among all. With an increase in holding time, a decrease in toughness has been reported. Samples B, C, and D have shown a decrement in the toughness by 10%, 25%, and 35% in comparison to the untreated sample.

REFERENCES

1. B. Roy, R. Kumar, J. Das: Materials Science & Engineering A, 631, 2015, 241-247. https://doi.org/10.1016/j.msea.2015.02.050.

2. R. Singh, S. Goel, R. Verma, R. Jayaganthan, A. Kumar: IOP Conf. Ser., Mater. Sci. Eng., 330, 2018, 012017. https://iopscience.iop.org/article/10.1088/1757-899X/330/1/012017.

3. P. Wang, Y. Zhang, D. Yu: Materials, 12, 2019, 290. https://doi.org/10.3390/ma12020290.

4. H.Y. Liou, W.T. Tsai, Y.T. Pan, R.I. Hsieh: J. of Materi Eng and Perform, 10, 2001, 231–241. https://doi.org/10.1361/105994901770345268.

5. K. Mumtaz, S. Takahashi, J. Echigoya, Lf. Zhang, Y. Kamada, M. Sato: Journal of Materials Science Letters, 21, 2002, 1199–1201. https://doi.org/10.1023/A:1016568402120.

6. S. Takahashi, J. Echigoya, T. Ueda, X. Li and H. Hatafuku: J. Materials Processing Technology, 108, 2001, 213-216. https://doi.org/10.1016/S0924-0136(00)00757-3.

7. *Metallographic preparation of stainless steel*. (Date of access: 07/03/2023): https://www.struers.com/en/Knowledge/Materials/Stainless-Steel#.

8. H. Essoussi, S. Elmouhri, S. Ettaqi, E. Essadiqi: Procedia Manufacturing, 32, 2019, 883–888. https://doi.org/10.1016/j.promfg.2019.02.298.

9. P. V. Reddy, B. V. Reddy, P. J. Ramulu: SN Applied Sciences, 2, 2020, 205. https://doi.org/10.1007/s42452-020-2026-7.

10. A. T. Zeuner, L. Ewenz, J. Kalich, S. Schöne, U. Füssel, M. Zimmermann: Metals, 12, 2022, 1514. https://doi.org/10.3390/met12091514.

11. J. W. Fu, Y. S. Yang, J. J. Guo, J. C. Ma, W. H. Tong: Materials Science and Technology, 25, 2009, 1013-1016. https://doi.org/10.1179/174328408X317093.

12. H. Li, L. Zhang, B. Zhang, Q. Zhang: Advances in Materials Science and Engineering, 2020, 1280761. https://doi.org/10.1155/2020/1280761.

13. X. Shi, K. Yang, M. Yan, W. Yan, Y. Shan: Frontiers in Materials, 7, 2020, 83. https://doi.org/10.3389/fmats.2020.00083.

14. V. Zatkalíková, M. Uhrícik, L. Markovicová, L. Kucharikov: Materials, 15, 2022, 8543. https://doi.org/10.3390/ma15238543.

15. X. Li, Y. Wei, Z. Wei, J. Zhou: IOP Conference Series: Earth and Environmental Science, 252, 2019, 022027. https://iopscience.iop.org/article/10.1088/1755-1315/252/2/022027.

16. H. Yoon, H. Ha, T. Lee, S. Kim, J. Jang, J. Moon, N. Kang: Metals, 9, 2019, 930. https://doi.org/10.3390/met9090930.

17. G. Bai, S. Lu, D. Li, Y. Li: Corrosion Science, 90, 2015, 347 – 358. http://dx.doi.org/10.1016/j.corsci.2014.10.031.

18. C. Huh, S. An, M. Kim, C. Kim: Applied Sciences, 9, 2019, 5557. https://doi.org/10.3390/app9245557.

19. A. V. Bansod, A.P. Patil, A.P. Moon, N.N. Khobragade: J. of Materi Eng and Perform, 25, 2016, 3615–3626. https://doi.org/10.1007/s11665-016-2221-2.

20. ASTM International. Standard Practices for Detecting Susceptibility to Intergranular Attack in Austenitic Stainless Steels. Available online: http://www.tdqs.ru/static/doc/astm_a262_15.pdf (Date of access: 15 May 2023).

21. F.J. Cárcel-Carrasco, M. Pascual-Guillamón, L. Solano García, F. Salas-Vicente, M.A. Pérez-Puig: Appl. Sci., 9, 2019, 3265. https://doi.org/10.3390/app9163265.

22. S. Tokuda, I. Muto, Y. Sugawara, N. Hara: J. Electrochem. Soc., 168, 2021, 091504. https://iopscience.iop.org/article/10.1149/1945-7111/ac28c6.

23. J. Zhan, M. Li, J. Huang, J, H. Bi, Q. Li, H. Gu: Metals, 9, 2019, 129. https://doi.org/10.3390/met9020129.